

# APPLICATION OF CRITICAL STRESS STATE CRITERION APPROACH TO FLEXURAL STRENGTHENED CONCRETE BEAMS USING FRP SHEETS

H. A. Toutanji<sup>a\*</sup>, R. Vuddandam<sup>b</sup>

<sup>a</sup>*Dept. of Civil and Env. Eng., Prof., University of Alabama in Huntsville, Huntsville, AL 35899*

<sup>b</sup>*Graduate Teaching Assistant, University of Alabama in Huntsville, Huntsville, AL 35899*

*\*toutanh@uah.edu*

**Keywords:** flexural strength, fiber reinforced polymer, externally bonded composite, reinforced concrete structures.

## Abstract

*For the past few years externally bonded fibre reinforced polymer (FRP) composites are used for strengthening existing reinforced concrete structures. The performance of the strengthened structures depends on the bond between concrete and FRP. To capture the debonding behavior for flexural strengthened concrete beams, prediction models have been developed considering equilibrium state of the four point bending beam and critical stress state of a concrete finite element in the vicinity of the bond interface expressed by the elasticity theory. The prediction expressions and critical stress state criterion are applied for a four point bending test data. Finally, comparison is done between existing prediction models from literature and the proposed prediction expression.*

## 1. Introduction

Fiber reinforced polymers (FRP) materials have been accepted as a commonly used method for strengthening conventional materials such as reinforced concrete (RC) structures [1-2]. Experimental and theoretical studies on externally bonded FRP reinforcement (EBR) to RC structures showed a significant improvement in flexural stiffness, load carrying capacity, ductility and durability. Nevertheless, usage of the EBR method has some design related issues. A noteworthy concern in design is considering the failure modes due to delamination - plate end (PE) debonding and intermediate crack-induced (IC) debonding, apart from the conventional failure modes – FRP rupture, crushing of concrete, concrete cover separation and yielding of steel before concrete crushing [2]. In recent years, more attention has been drawn to address the delamination failure.

PE debonding occurs due to flexural and vertical shear deformations of a beam, involves separation of the FRP plate at or near a plate end. Considerable researches [3-11] have been directed to investigate the plate end debonding. To avoid or delay plate end debonding, suitable anchorage systems were proposed by different researchers [12-14]. Anchorage systems were able to improve not only the strength, but also ductility of the structure [15] and

effectively delay plate end debonding. However, by providing mechanical anchors to pre-cracked beams in some scenarios have adverse effect in strength and also induces complex interfacial stresses affecting design assumptions.

IC debonding initiates near the interface of FRP and concrete substrate, wherever a flexural or flexural/shear crack intercepts the FRP plate. As the applied load increases, the IC interface crack rapidly propagates towards the plate end causing a brittle failure. The IC debonding was found to be more significant failure in single-span simply supported FRP plated reinforced concrete structures, due to high shear span-to-depth ratio and usage of thin FRP plate [16]. Although IC debonding is the important failure mode, there are few researches [17-20] focused on this debonding behavior. Considering a single crack, Niu and Wu [17], Teng et al [18-19] proposed analytical models assuming that shear stress transfer near flexural cracks is similar to that of simple shear tests. Aeillo and Ombres [20] developed a model based on moment-curvature relationships by considering a beam element between two adjacent cracks subjected to constant bending moment. All of these models [17-20] neglect the normal/peeling stresses where the interfacial normal stresses account for the vertical deformation compatibility between the bonded plate and the beam.

For the last decade, many studies focused on determination of interfacial stresses for the beams bonded with either steel or FRP plates. Smith and Teng [21] presented a comprehensive review of the available models and finally proposed a new model considering the drawbacks of the reviewed models. Recent studies [22-25] provided more accurate and improved solutions for interfacial stresses in which adherends shear deformations are taken into account. In this study, the flexural strength is determined theoretically by proposing a failure criterion where the maximum principal tensile stress on a small element in concrete substrate is limited to the tensile strength of concrete.

## **2. Load transfer at the bond interface**

### *2.1. Failure criteria for debonding*

To examine the bond system of FRP-to-concrete for flexural strengthened structures, four point bending test is widely adopted due to its simplicity. In the test, mechanical properties of FRP, concrete substrate, and adhesive are considered as important parameters. In this paper, thickness and tensile young's modulus of elasticity are denoted as  $t$  and  $E$  with subscripts  $p$  for FRP and  $a$  for adhesive (Fig. 1). FRP strip with the width  $b_p$  is attached to the soffit of the beam. The loading configuration parameters shown in Figure 1 are described by the width of the beam,  $b$ , the overall depth of the beam,  $h$ , the distance from the compression face to the centroid of tension side steel,  $d$ , the distance from the support to the nearer end of the soffit plate,  $a$ , the distance from the support to the nearest point load from the applied load,  $B$ , the span of the beam,  $L$  and the applied load,  $Q$ .

After the formation of flexure or flexure/shear crack, the crack at the interface propagates towards the nearest plate end. During crack propagation, only a part of interfacial stresses at the interface contribute to the bond strength [19]. This bonding zone along which most of the interfacial stresses transmitted into the concrete is called effective stress transfer length (ESL) or effective bond length (EBL) or simply effective length, denoted by  $L_e$ . The applied load  $Q$

is transmitted to concrete substrate near bond interface as interfacial shear and normal stresses with the distribution function of  $\tau(x)$  and  $\sigma_n(x)$ , respectively along the effective bond length,  $L_e$ . For simplicity, to identify a small element in concrete substrate, the edge of flexural crack is denoted as leading edge and far from leading edge up to which the interfacial stresses is dominant,  $L_e$  is denoted as trailing edge.

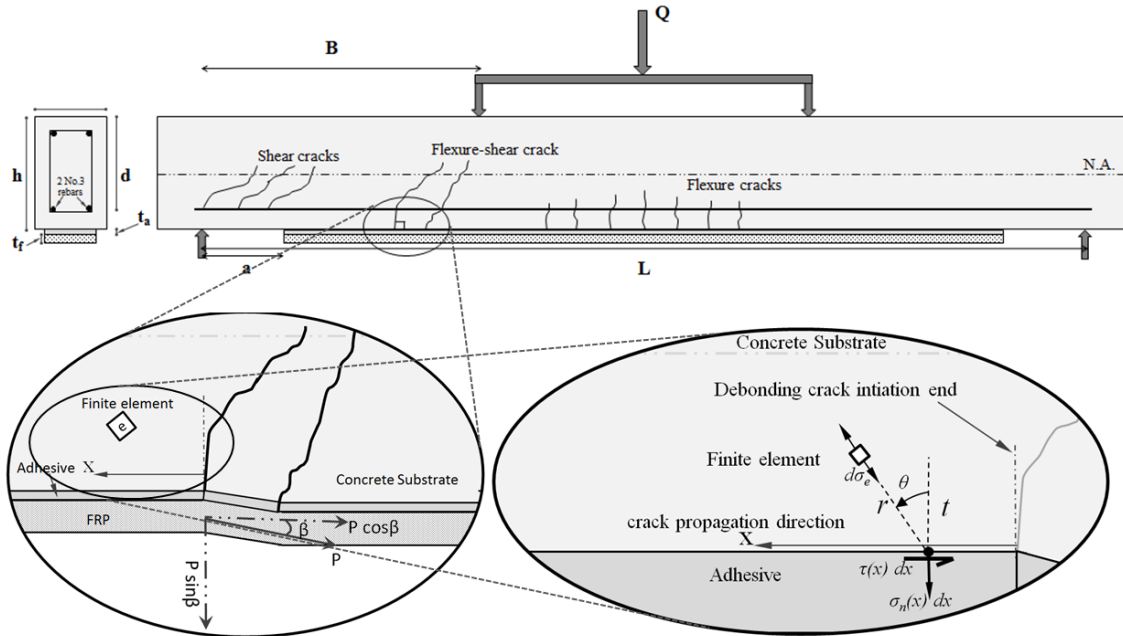


**Figure 1.** Sketch of four point bending test for FRP-to-concrete bond joint. Stress state of finite element in concrete substrate.

Several studies in their bond strength models [26-29] considered that crack propagation at the bond interface starts at a certain depth in concrete substrate. Yao et al. [30] reported, through experimental studies, that thin concrete layer attached to the debonded FRP strip and confirmed that its thickness is in the range of 1 to 5 mm. Thus, it is assumed that the initial fracture in FRP debonding occurs in concrete substrate elements below the bond interface at depth  $t$  and away from the leading edge at distance  $d$ . For maximum flexural strength, the maximum principal stress state on the small element in concrete substrate should not exceed its tensile strength  $f_t$ , and the failure criteria can be simply proposed as

$$\sigma_{1,d} \leq f_t \quad (1)$$

where  $\sigma_{1,d}$  = the maximum principal stress on small element of concrete substrate at depth  $t$  from the interface and distance  $d$  from the leading edge. The tensile strength of concrete in the unit of MPa can be obtained from ACI code [31] as a function of the cylindrical compressive strength  $f_c'$  (MPa) as:

$$f_t = 0.53f_c'^{0.5} \quad (2)$$

The maximum principal tensile stress on a small element is found by considering the biaxial stress state of the element and is given by

$$\sigma_{1,d} = \frac{(\sigma_x + \sigma_{n-e,d})}{2} + \sqrt{\left(\frac{\sigma_x - \sigma_{n-e,d}}{2}\right)^2 + \tau_{e,d}^2}, \quad (3)$$

where  $\sigma_x$  = the bending stress determined from flexural analysis;  $\sigma_{n-e,d}$  and  $\tau_{e,d}$  are the critical normal stress and critical shear stress respectively discussed more in the later sections of the present study.

## 2.2. Stress state in concrete substrate induced by interfacial shear and normal (peeling) stress

The elasticity theory derives the stress state on an element in the material subjected to both horizontal and vertical loads acting at the surface. The expression for the stress state, denoted  $d\sigma$ , is obtained as follows [32];

$$d\sigma = \frac{2 dH}{\pi r} \sin\theta + \frac{2 dV}{\pi r} \cos\theta, \quad (4)$$

where  $dH$  = the differential horizontal force on the material surface;  $dV$  = the differential vertical force on the material surface;  $r$  = the radial distance from the load applying point to the considered element;  $\theta$  = the angle measured from the vertical line to the radial line with the loading point as the origin in anti-clockwise positive.

For four point bending test, the expedient concentrated horizontal and vertical loads at a point are assumed as  $\tau(x)dx$  and  $\sigma_n(x)dx$  respectively. By these forces, a differential stress,  $d\sigma_e$ , is induced perpendicularly to a plane of a square finite element in concrete substrate shown in Figure 1. The differential stress on the element,  $d\sigma_e$ , induced by horizontal and vertical loads at any point along the bond length can be given by

$$d\sigma_e = \frac{\tau(x)dx}{\pi t} \sin 2\theta + \frac{\sigma_n(x)dx}{\pi t} (1 + \cos 2\theta), \quad (5)$$

where  $t$  = distance between the bond interface and embedded fracture surface;  $\theta$  = the angle measured from the vertical line of arbitrary  $x$  position to the radial line in anti-clockwise positive. It is noted that the positive differential stress means tensile stress.

On the same element, the infinite number of the differential stresses with different magnitudes and directions are superimposed due to consecutive horizontal and vertical loads on the concrete substrate surface. A conceptual interfacial shear and normal stress distributions along the length of a bonded FRP laminate is shown in Figure 2. The interfacial stresses from Equation 5 are complex as shear and normal stresses are coupled. Assuming FRP plate and the concrete beams have the same curvature [21], the shear and normal stresses can be uncoupled. For the critical stress state, all differential stresses are transformed with the Mohr's principle on to a certain plane, denoted as the critical plane. On an element at distance  $d$  from the leading edge and at depth  $t$ , the uncoupled critical shear stresses  $\tau_{e,d}$  and critical normal stresses  $\sigma_{n-e,d}$  can be expressed as

$$\tau_{e,d} = \int_0^{L_e} \frac{\tau(x)}{2\pi t} (1 + \cos 2\theta_1) \sin 2\theta_2 dx \quad (6)$$

$$\sigma_{n-e,d} = \int_0^{L_e} \frac{\sigma_n(x)}{2\pi t} (1 + \cos 2\theta_1)(1 + \cos 2\theta_2) dx, \quad (7)$$

where  $\theta_1$  = the transformation angle;  $\theta_2 = \tan^{-1} |x - d|/t$ ;  $L_e$  = effective bond length. Each differential stress is transformed to the critical plane by rotating its plane at  $\theta_1$  with the Mohr's stress transformation principle. The critical plane is determined as one with the critical differential stress, which is the angle  $\theta = \pi/4$ . When no plane with such angle exists, the plane with the differential stress by loads at the leading edge would be critical. Therefore, the expression for  $\theta_1$  is given by

$$\theta_1 = \begin{cases} \theta_2 - \theta_3, & d < t \\ \theta_2 - \frac{\pi}{4}, & d \geq t \end{cases} \quad (8)$$

where  $\theta_3 = \tan^{-1} (d/t)$ . In the case  $d < t$ , the considered element is relatively close to the leading end (Fig. 2a) and in the case  $d \geq t$ , the critical differential stress is evaluated with  $\theta_2 \geq \pi/4$  (Fig. 2b).

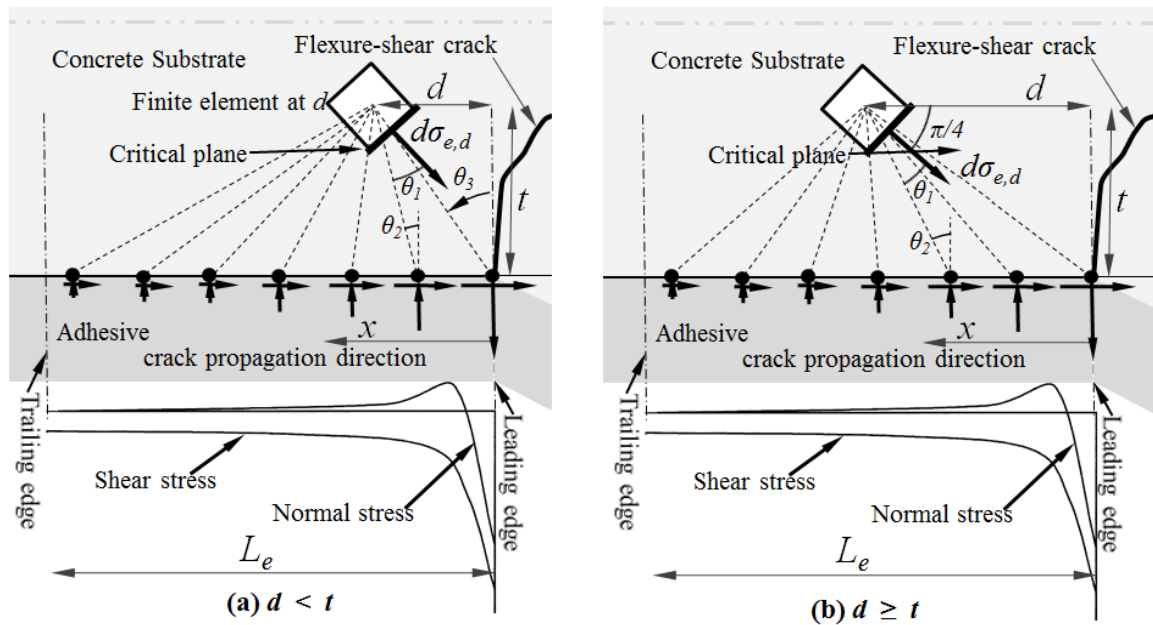


**Figure 2.** Conceptual interfacial shear and normal stresses along effective stress transfer length ( $L_e$ ); and Transformed stress on a critical plane. (a) case  $d < t$ ; and (b) case  $d \geq t$ .

### 3. Comparisons with existing models

As verification to the present solution, comparisons of the maximum principal stress from the present study with typical existing analytical solutions [21-22] are made. As an example, a reinforced concrete (RC) beam strengthened with thin carbon FRP plate is investigated. The strengthened beam is simply supported with two point loads. The span of the beam is  $L = 2300$  mm, the distance from the support to the end of the CFRP plate is  $a = 25$  mm, the applied load distributed symmetrically to the two point loads is  $Q = 60$  kN, and the distance from the support to the nearest point load is  $B = 767$  mm. A summary of geometric and material properties of the strengthened beam is given in Table 1.

Component	width [mm]	depth [mm]	Young's Modulus [GPa]	Poisson's Ratio	Shear Modulus [GPa]
RC beam	b=200	h=225	E <sub>c</sub> =31	0.18	G <sub>c</sub> =13.14
Adhesive layer	b <sub>a</sub> =200	t <sub>a</sub> =2	E <sub>a</sub> =2	0.35	G <sub>a</sub> =1.11
CFRP plate	b <sub>f</sub> =200	t <sub>f</sub> =4	E <sub>f</sub> =100	0.28	G <sub>f</sub> =5

**Table 1.** Geometric and material properties.

The peak interface shear and interface normal stresses using existing models [21-22] are shown in Table 2. A MATLAB program was written to identify the critical element through iteration process. The peak stresses on the critical element obtained from present study are the critical shear and critical normal stresses, and the corresponding maximum principal stress (Table 2). As expected, it is identified that peak critical normal stress is lesser than peak interfacial normal stress due to effect of differential (compressive normal stress and tensile normal stress) stresses on a critical finite element.

Component	Interfacial shear stress	Interfacial normal stress	Critical shear stress	Critical normal stress	Maximum principal stress
	$\tau$ [MPa]	$\sigma$ [MPa]	$\tau_{e,d}$ [MPa]	$\sigma_{n-e,d}$ [MPa]	$\sigma_{l,d}$ [MPa]
Smith & Teng [21]	2.94	1.56	3.50	0.96	4.07
Tounsi [22]	1.42	0.84	2.07	0.58	2.45

**Table 2.** Comparison of peak interfacial normal stress, shear stresses Vs proposed critical normal stress, critical shear stress and maximum principal stress.

#### 4. Conclusions

In this study, a critical stress state criterion is proposed based on the theory of elasticity. Critical stress criterion is developed considering that crack propagation occurs at the bond interface at a certain depth in concrete substrate. The interface stresses developed by several studies are valid at the interface. In present study, a critical finite element is first identified along the effective stress transfer length. Then the differential stresses at the interface are transformed on to a critical plane of the finite element using Mohr's principle. Finally, considering the biaxial stress state of the critical finite element, maximum principal stress is determined for the obtained critical shear and normal stresses. For design, a criterion is proposed that the maximum principal stress is limited to tensile strength of the concrete.

#### References

- [1] G. J. Teng, F. J. Chen, T. S. Smith and L. Lam. *FRP strengthened RC structures*. John Wiley & Sons Ltd, Chichester, UK, 2002.
- [2] L. C. Hollaway and J. G. Teng. *Strengthening and rehabilitation of civil infrastructures using fiber reinforced polymer (FRP) composites*. Woodhead Publishing Limited, Cambridge, UK, 2008.
- [3] D. J. Oehlers and J. P. Moran. Premature Failure of Externally Plated Reinforced Concrete Beams, *Journal of Structural Engineering*, ASCE, 116(4): 978-995, 1996.
- [4] M. Raof and S. Zhang. Analysis of plate peeling failure of RC beams with externally bonded plates, *Proceedings of the International Conference on Concrete in the Service of mankind: Concrete Repair Rehabilitation and Protection*, University of Dundee,

- Scotland, UK, 24-26 June 1996, Dhir and Jones (Eds), E & FN Spon, pages 605-614, 1996.
- [5] W. Jansze. Strengthening of reinforced concrete members in bending by externally bonded steel plates, *PhD thesis*, Delft University of Technology, 1997.
- [6] H. Saadatmanesh and A. M. Malek. Design guidelines for flexure strengthening of RC beams with FRP plates. *Journal of Composites for Construction*, ASCE, 2(4): 158-164, 1998.
- [7] O. Ahmed and D. van Gemert. Effect of longitudinal carbon fibre reinforced plastic laminates on shear capacity of reinforced concrete beams. *Proceedings of the 4th International Symposium on Fibre Reinforced Polymer Reinforcement for Reinforced Concrete Structures*, Baltimore, Maryland, USA, Dolan et al. (eds), pages 933-943, 1999.
- [8] M. Raouf and M. A. H. Hassanen. Peeling failure of reinforced concrete beams with fibre reinforced plastics or steel plates glued to their soffits. *Proceedings of the institution of Civil Engineers: Structures and Buildings*, 140: 291-305, 2000.
- [9] S. T. Smith and J. G. Teng. FRP strengthened RC beams – I: Review of debonding strength models. *Engineering Structures*, 24(4): 385-395, 2002.
- [10] S. T. Smith and J. G. Teng. FRP strengthened RC beams – II: assessment of debonding strength models. *Engineering Structures*, 24(4): 397-417, 2002.
- [11] J. G. Teng and J. Yao. Plate end debonding in FRP plated RC beams-II: strength model. *Engineering Structures*, 29(10): 2472-2486, 2007.
- [12] A. Sharif, F. J. Al-Sulaimani, I. A. Basunbul, and M. H. Baluch. Strengthening of initially loaded reinforced concrete beams using FRP plates, *ACI Structural Journal*, 91(2): 160-168, 1994.
- [13] G. Spadea, F. Bencardino and R. N. Swamy. Optimizing the performance characteristics of beams strengthened with bonded CFRP laminates, *Materials and Structures*, RILEM, 33(226): 119-126, 2000.
- [14] A. J. Lamanna, L. C. Bank and D. W. Scott. Flexure strengthening of reinforced concrete beams by mechanically attaching fibre-reinforced polymer strips. *Journal of Composite for Construction*, ASCE, 8(3): 203-210, 2004.
- [15] F. Ceroni and M. Pecce. Evaluation of bond strength in concrete element externally reinforced with CFRP sheets and anchoring devices. *Journal of Composite for Construction*, ASCE, 14(5):521-530, 2010.
- [16] W. M. Sebastian. Significance of midspan debonding failure in FRP-plated concrete beams. *Journal of Structural Engineering*, 127(7): 792-798, 2001.
- [17] H. Niu and Z. Wu. Peeling-off criterion for FRP-strengthened RC flexural members, in: Teng JG., (Ed.) *Proceedings of the International Conference on FRP Composites in Civil Engineering*, Hong Kong, pages 571–578, 2001.
- [18] J. G. Teng, S. T. Smith, J. Yao and J. F. Chen. Strength model for intermediate flexural crack induced debonding in RC beams and slabs, in: Teng JG. (Ed.), *Proceedings of the International Conference on FRP Composites in Civil Engineering*, Hong Kong, pages 579–587, 2001.
- [19] J. G. Teng, S. T. Smith, J. Yao and J. F. Chen. Intermediate crack-induced debonding in beams and slabs. *Construction and Building Materials*, 17(6–7):447–62, 2003.
- [20] M. Aiello and L. Ombres. Cracking and Deformability Analysis of Reinforced Concrete Beams Strengthened with Externally Bonded Carbon Fiber Reinforced Polymer Sheets. *Journal of Materials in Civil Engineering*, 16(5): 392–399, 2004.
- [21] S. T. Smith and J. G. Teng. Interfacial stresses in plate beams. *Engineering Structures*, 23(7):857–71, 2001.

- [22] A. Tounsi. Improved theoretical solution for interfacial stresses in concrete beams strengthened with FRP plate. *International Journal of Solids and Structures*; 43:4154–4174, 2006.
- [23] P. Qiao and F. Chen. An improved adhesively bonded bi-material beam model for plated beams. *Engineering Structures*, 30(7):1949–1957, 2008.
- [24] V. Narayanamurthy, J. F. Chen, J. Cairns and A. Ramaswamy. Effect of shear deformation on interfacial stresses in plated beams subjected to arbitrary loading. *International Journal of Adhesion & Adhesives*, 31:862–874, 2011.
- [25] B. Guenaneche, A. Tounsi and E. Adda bedia. Effect of shear deformation on interfacial stress analysis in plated beams under arbitrary loading. *International Journal of Adhesion and Adhesives*, 48:1-13, 2014.
- [26] O. Buyukozturk, O. Gunes and E. and Karaca. Progress on understanding debonding problems in reinforced concrete and steel members strengthened using FRP composites. *Construction and Building Materials*, 18(1):9–19, 2004.
- [27] X. Z. Lu, J. G. Teng, L. P. Ye and J. J. Jiang. Bond–slip models for FRP sheets/plates bonded to concrete. *Engineering Structures*, 27(6):920–937, 2005.
- [28] W. Yefei, Z. Zhou, Q. Yang and W. Chen. On shear bond strength of FRP-concrete structures. *Engineering Structures*, 32(3):897–905, 2010.
- [29] K. Brosens. Anchorage of externally bonded steel plates and CFRP laminates for the strengthening of concrete elements. *PhD thesis*, Katholieke Universiteit Leuven, Leuven, 2001.
- [30] J. Yao, G. J. Teng and F. J. Chen. Experimental study on FRP-to-concrete bonded joints. *Composites: Part B*, 36:99-113, 2005.
- [31] American Concrete Institute (ACI). *Building code requirements for structural concrete*. ACI 318-11, Farmington Hills, Michigan, 2011.
- [32] A. C. Uğural and S. K. Fenster. *Advance Strength and Applied Elasticity*. 4th edition, Prentice Hall, 2003.
- [33] American Concrete Institute (ACI), *Guide for the Design and Construction of Externally Bonded FRP Systems for Strengthening Concrete Structures*, ACI 440.2R-08, ACI, Farmington Hills, Michigan, 2008.